

Adsorption of block polyampholyte micelles in monolayers at the silicon water interface

B. Mahltig⁽¹⁾, J.-F. Gohy⁽²⁾, R. Jérôme⁽²⁾, C. Bellmann⁽³⁾, M. Stamm⁽³⁾

⁽¹⁾Max-Planck-Institut für Polymerforschung Ackermannweg 10, 55128 Mainz Germany

⁽²⁾Centre for Education and Research on Macromolecules, University of Liège, Sart-Tilman B6, 4000 Liège Belgium

⁽³⁾Institut für Polymerforschung Dresden e.V., Hohe Strasse 6 01069 Dresden Germany

Abstract

The adsorption of the diblock polyampholyte poly(methacrylic acid)-*block*-poly((di-methylamino)ethyl methacrylate) from aqueous solution on silicon substrates was investigated as a function of polymer concentration and pH. Dynamic light scattering and electrokinetic measurements were used to characterize the poly-ampholyte in solution. The amount of polymer adsorbed was determined by ellipsometry and lateral structures of the polymer layer were investigated by scanning force microscopy. The amount of polymer adsorbed was found to be strongly influenced by the pH of the polymer solution, while the size of the poly-ampholyte micelles adsorbed on the surface was hardly affected by pH during adsorption. From investigations by scanning force microscopy well-separated micelles were seen in the dried monolayers adsorbed directly from solution. The structures at the surface are correlated to structures in solution, and the adsorbed amount depends on the relative charge of the micelles and the surface.

Key words: Polyampholytes - Ellipsometry - Force microscopy - Adsorption - Micelles

1. Introduction

Polyampholytes are highly charged polymers quite similar to polyelectrolytes, except that polyampholytes consist of oppositely charged structural units. Adsorption processes of polyelectrolytes and polyampholytes at solid/liquid interfaces have been studied intensively in the last few years [1-3]. The strong interest in this topic results from the large variety of practical applications, for example, paper production, wastewater treatment and washing powder [4-7].

Numerous studies have treated polyelectrolytes in solution and at solid/liquid interfaces [8-17]. Adsorption of amphiphilic diblock copolymers with a charged hydrophilic and an uncharged hydrophobic polymer block is also reported in the literature [18-21]. These polymer systems form micelles in solution and the adsorption of entire micelles is observed. While the behaviour of polyampholytes in solution has also been the topic of several articles [22-24], their adsorption has rarely been discussed [25-29].

We investigated polymer adsorption from a solution of the diblock polyampholyte poly(methacrylic acid)-*block*-poly((dimethylamino)ethyl methacrylate) (PMAA-*b*-PDMAEMA) onto silicon surfaces. The adsorbed polymer layers were investigated by ellipsometry and scanning force microscopy (SFM). The behaviour of this polyampholyte in solution was investigated by dynamic light scattering (DLS) and electrokinetic measurements. In contrast to previous studies [30, 31] we observed by ellipsometry a high adsorbed amount, which is strongly influenced by the pH of the polyampholyte solution. The maxima in adsorption were found at the isoelectric point (IEP) of the polymer. Our investigations with DLS in solution and SFM at the dry adsorbed polymer layers indicated that the high adsorbed amount is caused by the adsorption of entire micelles. The combination of different methods demonstrated that the polyampholyte micelles adsorb in monolayers.

While the pH of the polyampholyte solution was found to have a strong influence on the adsorbed amount, the size of the micelles is hardly affected by pH in the area where the main adsorption takes place.

2. Materials and methods

2.1. Diblock polyampholyte

For the adsorption experiments we used the ampholytic diblock copolymer PMAA-*b*-PDMAEMA (Fig. 1). The molecular weight was 62000 g/mol and the weight ratio of the blocks PMAA to PDMAEMA was 19:81. The polyampholyte was synthesized by a sequential anionic copolymerization as described in the literature [32-34]. The molecular weight and the block size were determined by gel permeation chromatography and ¹H NMR

spectroscopy, respectively. The IEP of the polyampholyte in solution, determined by electrokinetic measurements, was pH 9.3. Precipitation of the polyampholyte was not observed in the pH range studied.

2.2. Adsorbent

Silicon wafers with a native oxide layer of typically 2 nm thickness were used. Prior to the adsorption experiments, the wafers were cleaned and treated such that the IEP of the surface was pH 3.8, as determined by streaming potential measurements. First the wafers were cleaned with dichloromethane in an ultrasonic bath at 40°C for 15 min. After washing with Millipore water, the wafers were put into an oxidation bath of H₂O₂, NH₃ and Millipore water for 30 min at 70°C. Finally, the wafers were rinsed with Millipore water again and were dried with nitrogen.

2.3. Polymer adsorption

The adsorption of the polyampholyte on the silicon substrates was carried out by treating the substrates with an aqueous solution of the polyampholyte containing 0.01 mol/l NaCl. The polymer concentration and pH were varied from 0.00061 g/l to 0.549 g/l and from 3.3 to 11.6, respectively. The pH was adjusted with NaOH and HCl in amounts negligible compared to the salt concentration.

Prior to the experiment the solution was stirred for 20 s. The silicon wafer was exposed to the polymer solution for more than 12 h, which is sufficient time to reach equilibrium of adsorption. Afterwards the wafer was taken out of the solution and washed with Millipore water for a few seconds to remove any loosely attached residues.

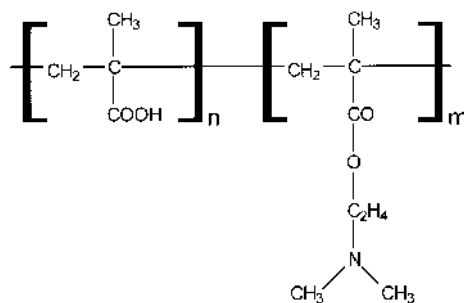


Fig. 1 Schematic drawing of the structural units of the polyampholyte: poly(methacrylic acid) left and poly((dimethylamino)ethyl methacrylate) right

Kinetic measurements of the adsorption process were performed in situ in a specially designed Teflon cell by ellipsometry [35]. The cell was filled with water containing 0.01 mol/l NaCl and the constancy of the ellipsometer readings with time was checked. After reaching constant values, the adsorption process was started by the injection of the polymer dissolved in Millipore water. After the injection the solution was stirred for 20 s. Ellipsometric angles were recorded every 20 s.

2.4. Ellipsometry

Ellipsometry was used to determine the amount of the polyampholyte adsorbed on the silicon wafers. All measurements were performed using a computer-controlled null-ellipsometer in a vertical polarizer-compensator-sample-analyser arrangement [35]. To obtain the best sensitivity the angle of incidence was fixed at 70°. A He-Ne laser with a wavelength of 632.8 nm was used as a light source.

The ellipsometric angles ψ and Δ were calculated from the polarizer, p , and analyser, a , settings at the minima of the signal intensity: $\psi = 2p + 90$ and $\Delta = a$ [36]. From these measurements, p and a in zone I and zone III were determined to obtain average values of ψ and Δ [37].

The thickness, d , of the adsorbed polymer layer was calculated from the ellipsometric angles using a multilayer model [36]. Our layer system consisted of an adsorbed polymer film in contact with air or an aqueous polymer solution on a silicon oxide layer, which is located on the silicon wafer.

The amount of polymer adsorbed, A , is given for dried samples measured in air by the mass density, ρ , of the polymer and the measured thickness,

$$d \cdot A = \rho \cdot d \quad (1)$$

For measurements in an aqueous solution the adsorbed amount was calculated using the following equation [38].

$$A = \frac{d(n_1 - n_0)}{dn/dc} \quad (2)$$

n_1 and n_0 are the refractive indices of the polymer layer and the polymer solution, $dn/dc = 0.1246$ ml/g is the increment of the refractive index of the polymer.

2.5. Electrokinetic measurements

Electrophoretic measurements were used to determine the IEP of the polyampholyte in solution. For these measurements a commercially available Zeta Sizer 3 (Malvern Instruments, UK) was used. Based on the Smoluchowski equation, the electrophoretic mobilities were converted to the zeta potential. To determine the zeta potential as a function of pH, 1 mol/l HCl and 1 mol/l KOH were used to adjust the pH of the polymer solution. The pH, where the zeta potential is found to be zero, is the IEP of the polyampholyte [39]. To maintain a constant electrical double layer thickness, all zeta potential measurements were carried out in 10^{-3} mol/l NaCl solutions.

The IEP of the cleaned silicon wafers was determined by streaming potential measurements with an electrokinetic analyser (EKA, Anton Paar, Austria). The electrical potential was measured as a function of pressure loss in a streaming channel between two plates. The correlation between the zeta potential and the streaming potential, U_s is given by [40]

$$U_s = \frac{\zeta c \epsilon_0 q \Delta p}{\eta l R} \approx \frac{\zeta c \epsilon_0 \Delta p}{\eta \chi} \quad (3)$$

with the relative dielectric constant ϵ_r , the absolute dielectric constant ϵ_0 , the pressure difference Δp , the viscosity η , the electrical resistance R , and the electrical conductance $\chi = I$ and q are the channel length and the cross-sectional area, respectively. To determine the zeta potential as a function of the pH the same conditions as for electrophoresis were used.

2.6. Dynamic light scattering (DLS)

DLS was used to determine the size of individual polyampholyte chains and the dimensions of the micelles in solution. The scattering system was built up from a commercial ALV 3000 digital correlator with a 400-mW krypton laser ($\lambda = 647$ nm) as a light source. All investigations were performed at room temperature. The measurements of the autocorrelation functions were performed at several pH. The polyampholyte concentration was set to 0.128 g/l and the salt concentration was 0.01 mol/l NaCl.

The analysis of the autocorrelation function gives the diffusion coefficient, from which the size of the polyampholyte in solution was calculated using the Stokes-Einstein relationship [41, 42]. Every sample was investigated at different scattering angles from 50° to 130° . No trend of the measured polyampholyte size as a function of the scattering angle was detectable. Therefore, the reported polymer size was calculated as the mean value from the measurements at different scattering angles.

2.7. Scanning Force Microscopy (SFM)

The topography of the dried adsorbed films was studied by SFM with a commercially available scanning force microscope (Autoprobe CP, Park Scientific Instruments). A red laser beam strikes a cantilever and the deflections of the laser caused by the moving cantilever are detected with a four-section photodetector. So the degree of motion of the cantilever can be detected from the difference in light intensity on the detector sections. The cantilevers were made from gold-coated silicon.

All investigations were performed in noncontact mode to minimize the damage to the polymer layers in the frequency range 72-76 kHz, depending on the individual tip resonance. To ensure reproducibility, the samples were scanned in different scanning areas from $2.5 \times 2.5 \mu\text{m}^2$ to $20 \times 20 \mu\text{m}^2$ at different positions on the sample. To compare the surface topography probed by SFM in a less pictorial way, the SFM images were analysed with the following procedure. First the Fourier transform of the individual SFM image was calculated. To get a better signal-to-noise ratio we calculated in a next step the power spectral density (PSD) from the Fourier

transform: $\text{PSD} = \frac{1}{2\pi} |F(q)|^2$ [43]. An example of a PSD, together with a SFM topography and the related two-dimensional Fourier transform, is shown in Fig. 2. If the PSD contains a peak, its position, s^* , was extracted by a fit of a Gaussian line shape to the PSD [44]. The dominant length scale, A , of our topography was then calculated from the position s^* :

$$= 1/s^* \quad (4)$$

In the case where the PSD shows a shoulder instead of a peak, the s^* was determined as the crossing point of two linear fits at the shoulder. For every sample s^* was obtained from images of different sizes and to calculate A the average of s^* was taken.

3. Results and discussion

3.1. pH dependence of adsorption

We carried out the polyampholyte adsorption in a pH range of 3.3—11.6. For all these experiments, the polyampholyte concentration was set to 0.128 g/l. The amount of polyampholyte adsorbed was strongly influenced by the pH of the solution (Fig. 3). The adsorption curve can be divided into four areas.

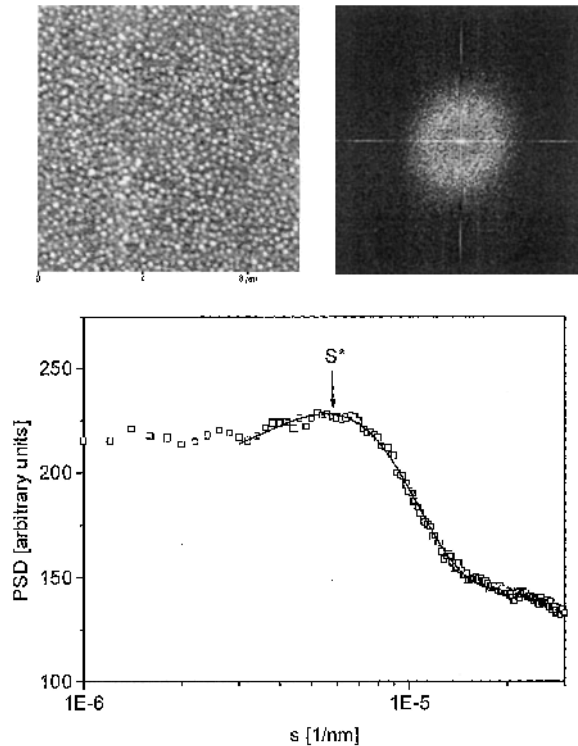


Fig. 2 $10 \times 10 \mu\text{m}^2$ scanning force microscopy (SFM) image together with the corresponding two-dimensional fast Fourier transform and power spectral density (PSD)

Below pH 3.8, both the polymer and the silicon substrate contain the same positive net charge and almost no adsorption was found. From pH 3.8 to 8.5, a small increase in the adsorbed amount to nearly $A = 3 \text{ mg/m}^2$ was observed. The area around the IEP of the polyampholyte at pH 9.3 is characterized by a strong increase in the adsorbed amount to a maximum of $A = 15 \text{ mg/m}^2$. Above pH 10 almost no adsorption took place.

This adsorption behaviour with a maximum adsorption at the IEP of the polyampholyte **was** recently found for different polyampholyte systems [1, 25, 28]. The electrostatic interaction between the strong negatively charged silicon substrate and the positively charged polyampholyte block is the driving force of the adsorption [11]. On approaching the IEP, the number of charges in the polyampholyte decreases, which leads to a screening of electrostatic repulsion between the adsorbing polyampholyte segments as well. Therefore, the polymer can adsorb at a higher density, which causes a larger amount to be adsorbed [30, 45].

3.2. Adsorption as a function of polyampholyte concentration

The adsorbed amount as a function of the polyampholyte concentration was investigated at different pH values above, below and directly at the IEP of the polyampholyte (Fig. 4). In every case the adsorption isotherms reached equilibrium at low polymer concentration and could be fitted by the adsorption model of Langmuir [46]. The Langmuir model is based on the adsorption of monolayers and describes the adsorbed amount, $A(c_p)$, as a function of the polymer concentration, c_p .

$$A(c_p) = A_{\infty} \left(\frac{Kc_p}{1 + Kc_p} \right), \quad (5)$$

where A_{∞} is the adsorbed amount at infinitely high polyampholyte concentration and $K = k_{ads}/k_{des}$ is the ratio of the rate of adsorption and desorption of the polyampholyte chains. From this behaviour, the adsorption of the polyampholyte in monolayers even at the IEP may be deduced.

The monolayers are, however, laterally inhomogeneous and will be discussed later in more detail.

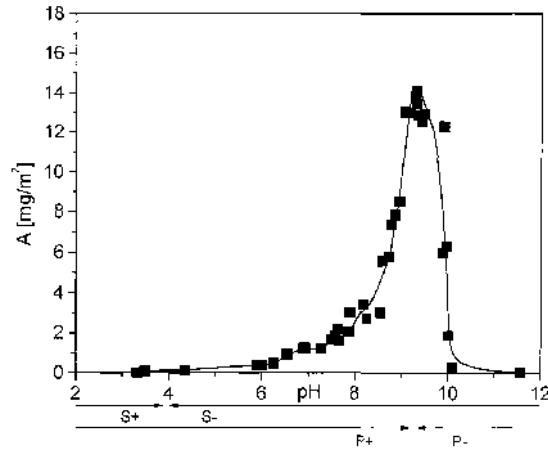


Fig. 3. Amount of polyampholyte adsorbed, A , as a function of pH (solid squares). The polymer concentration was set to 0.128 g/l. The solid line is a guide for the eye. The arrows indicate where the silicon surface and the polyampholyte carry a positive (S+, P+) or a negative (S-, P-) net charge

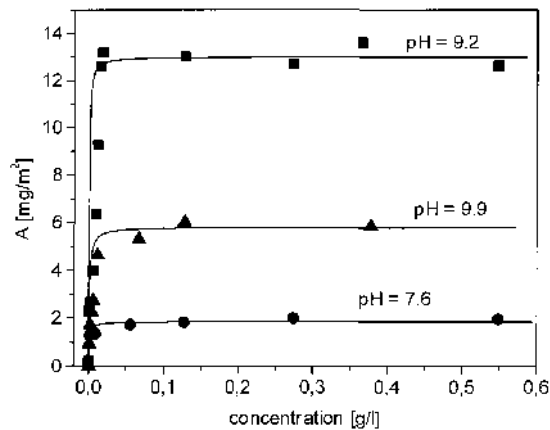


Fig. 4 Amount of polyampholyte adsorbed as a function of polyampholyte concentration at different pH values. The solid lines are fits based on the Langmuir adsorption model

3.4. Adsorption kinetics

The adsorption kinetics was investigated in situ by time resolved ellipsometry. The measurements were carried out in a range of pH and at a polyampholyte concentration of 0.128 g/l (Fig. 5). In every case the adsorbed amount reached a plateau value after a characteristic time depending on the pH. This behaviour agrees with the adsorption of monolayers. In the case of a low adsorbed amount, $A < 3 \text{ mg/m}^2$, the plateau is reached after some minutes. For the adsorption of higher amounts, $A = 7.0 \text{ mg/m}^2$ and 12.8 mg/m^2 , the first 4 mg/m^2 was also reached in some minutes but the adsorption of the remaining polymer required 2 h.

The rapid adsorption at the beginning results from the strong electrostatic interactions of the negatively charge silicon substrate and the positively charged polyampholyte block. The adsorption of additional polymer was governed by the penetration of polymer through the polymer already adsorbed [35]. Furthermore, the polymer already adsorbed shields the negative charge of the silicon substrate and this decreases the electrostatic interactions between the substrate and the polyampholyte in solution.

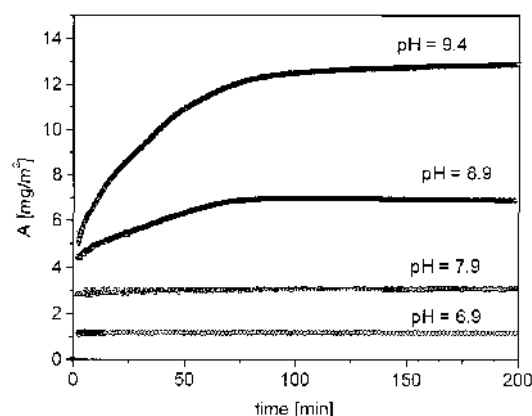


Fig. 5 Amount of polyampholyte adsorbed as a function of adsorption time at different pH values. The polymer concentration was set to 0.128 g/l

3.5. Lateral structures of the adsorbed polyampholyte

The lateral structures of dried adsorbed polyampholyte on silicon surfaces were investigated using SFM (Fig. 6). The adsorption was performed from solutions with different pH and at the same polymer concentration of 0.128 g/l.

The surface consists of lateral, round structures. The dominant length scale determined from PSD was assigned to the lateral diameter of these structures. From the PSD a high regularity of the lateral size was confirmed. The structures were sufficiently isolated from each other, if the adsorption was carried out at pH 6.9, 8.7 or 9.0. In the case of pH 6.9 the structures were approximately 200 nm in diameter, which is nearly double the size observed at pH 9.4.

Analogous behaviour was obtained from DLS for the size of polyampholyte micelles in solution (Fig. 7). In solution, micelles with a similar size as the adsorbed structures were observed. The micelle diameter decreases in solution from approximately 208 nm at pH 3.5 to approximately 84 nm at pH 9.4. The correlation of the micelle size in solution and of the adsorbed structures is explainable by the adsorption of whole micelles instead of single chains [20, 21]. The small thickness of adsorbed structures of only 25 nm in comparison with the larger lateral size is caused by the collapse of the adsorbed micelles during the drying of the sample [19].

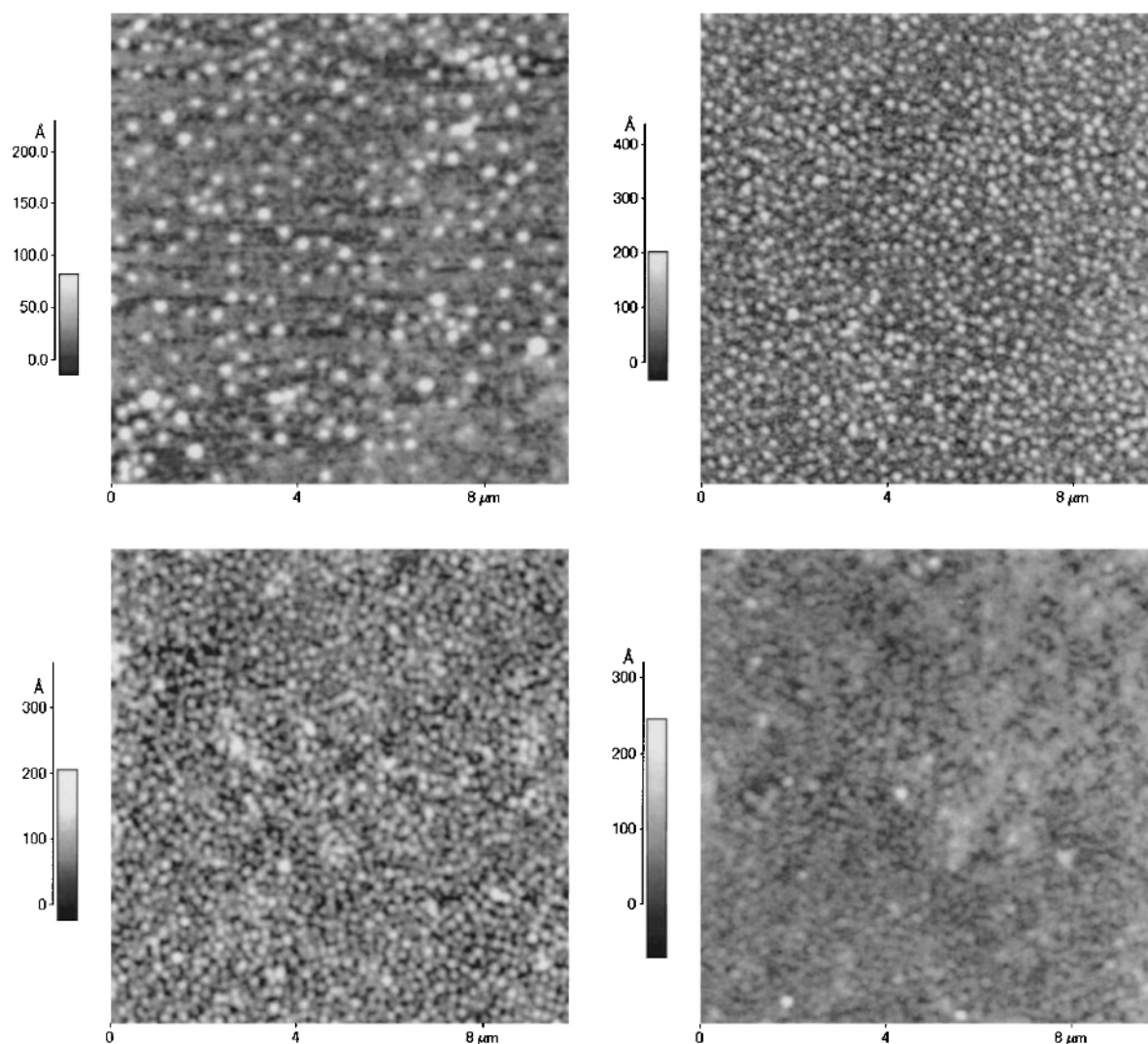


Fig. 6 SFM images of polyampholyte adsorbed on silicon substrates at a scan area of $10 \times 10 \mu\text{m}^2$. The polymer was adsorbed from solutions with different pH and the polyampholyte concentration was 0.128 g/l. The amount adsorbed measured by ellipsometry is given: top left: pH 6.9, $A = 1.2 \text{ mg/m}^2$; top right: pH 8.7, $A = 5.6 \text{ mg/m}^2$, bottom left: pH 9.0, $A = 8.5 \text{ mg/m}^2$; bottom right: pH 9.4, $A = 12.8 \text{ mg/m}^2$

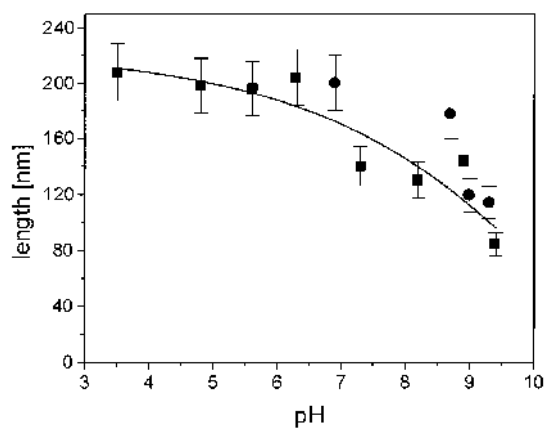


Fig. 7 Hydrodynamic diameter of the polyampholyte micelles in solution as a function of pH (solid squares). The dominant length scale of the SFM topographs of polyampholyte on silicon oxide prepared at different pH (solid circles). The solid line is a guide for the eye

Both the adsorption behaviour at different polymer concentrations and the kinetic measurements suggest the adsorption of micelles in monolayers. From these observations it was assumed that whole micelles adsorb as they are present in solution and that only monolayers of micelles build up.

While the adsorbed amount increases with pH between 6.9 and 9.4, the adsorbed micelles show only a small change in lateral size and nearly the same maximum height. The increase in the adsorbed amount was caused by a decrease in the distance between the micelles in the monolayer. Thus, the adsorbed amount was only determined by the distance and not by the size of the micelles. The decrease in distance towards the IEP of the polyampholyte was due to the decrease in the charge of the polyampholyte. Micelles with less charge exhibited less repulsive electrostatic interaction between each other. This allowed a higher density of adsorbed micelles on the substrate.

The polymer film adsorbed at pH 9.4, close to the IEP, showed less regular structures than the other three films investigated (Fig. 6). Due to the zero net charge at the IEP, the repulsive interaction of the micelles reached a minimum, allowing the micelles to adsorb at the highest density and to come in direct contact with each other. Thus, coagulation was possible and may explain the formation of structures with different sizes as well as the maximum in the adsorbed amount.

4. Conclusions

The adsorption of the polyampholyte PMAA-*b*-PDMA-EMA with a block size of 19:81 was investigated by means of ellipsometry, SFM, DLS and electrokinetic measurements. The adsorption from different solutions was studied as a function of pH, polyampholyte concentration and adsorption time. The adsorbed amount as a function of polymer concentration fits to the Langmuir model, and the adsorption reaches a plateau value after 2 h. This adsorption behaviour suggested that the polyampholyte adsorbed in monolayers. The SFM investigations on dry polymer substrates showed lateral, round structures. These regular and well-separated structures were explained by the adsorption of whole micelles, which had already formed in the polymer solution.

In the region where adsorption was strongly influenced by pH the size of the micelles was only insignificantly influenced by pH. The increase in adsorption towards the IEP was therefore explained by a decrease in the distance of the adsorbed micelles, until the converge at the IEP reached the maximum. The increase in the adsorbed amount results from a decrease in the net charge of the micelles, which causes a smaller electrostatic repulsion of the adsorbed micelles. Less repulsion leads to an adsorption at higher density.

It was concluded that the polyampholyte was adsorbed as a monolayer of micelles onto the silicon substrate. The monolayer was composed of well-separated micelles with a high degree of regularity. It was demonstrated that the spacing between the adsorbed micelles could be controlled by the solution pH.

Acknowledgements

We thank B. Silier and S. Wiegand for their help with DLS measurements. For helpful discussions we thank H. Walter and D. Collins. This work was supported by the DFG Schwerpunkt "Polyelektrolyte" (grant IIC10-322 1009). J.F.G. and R.J. are grateful to the Services Fédéraux des Affaires Scientifiques, Techniques et Culturelles for general support in the frame of Poles d'Attraction Interuniversitaires: PAI 4-11.

References

- [1] Cohen Stuart MA, Fler GJ, Lyklema J, Norde W, Scheutjens JM (1991) *Adv Colloid Interface Sci* 34:477
- [2] Förster S, Schmidt M (1995) *Adv Polym Sci* 120:51
- [3] Kudaibergenov SE (1999) *Adv Polym Sci* 144:115
- [4] Dautzenberg H, Jaeger W, Kötzt J, Philipp B, Seidel C, Stscherbina D (1994) *Polyelectrolytes*. Hanser, Munich
- [5] Watanabe Y, Kubo K, Sato S (1999) *Langmuir* 15:4157
- [6] Bôhm N, Kulicke W-M (1997) *Colloid Polym Sci* 275:73
- [7] Janex ML, Chaplain V, Counord JL, Audebert R (1997) *Colloid Polym Sci* 275:352
- [8] Blaakmeer JM, Bôhmer MR, Cohen Stuart MA, Fler GJ (1990) *Macro-molecules* 23:2301
- [9] Pefferkorn E, Jean-Chronberg AC, Varoqui R (1990) *Macromolecules* 23:1735
- [10] Hoogeveen NG, Cohen Stuart MA, Fler GJ (1994) *Faraday Discuss* 98:161
- [11] Dobrynin AV, Rubinstein M, Joanny J-F (1997) *Macromolecules* 30:4332
- [12] Skouri M, Munch JP, Candau SJ, Neyret S, Candau F (1994) *Macromolecules* 27:69
- [13] Zhang Y, Tirrell M, Mays JW (1996) *Macromolecules* 29:7299
- [14] Sukhishvili SA, Granick S (1998) *J Chem Phys* 109:6861
- [15] Shubin V, Linse P (1995) *J Phys Chem* 99:1285

- [16] Lee EM, Kanelleas D, Milnes JE, Smith K, Warren N, Webberly M, Rennie AR (1996) *Langmuir* 12:1270
- [17] An SW, Thirtle PN, Thomas RK, Baines FL, Billingham NC, Armes SP, Penfold J (1999) *Macromolecules* 32:2731
- [18] Meiners JC, Elbs H, Ritzi A, Mlynek J, Krausch G (1996) *J Appl Phys* 80:2224
- [19] Spatz JP, Sheiko S, Möller M (1996) *Macromolecules* 29:3220
- [20] Meiners JC, Quintel-Ritzi A, Mlynek J, Elbs H, Krausch G (1997) *Macromolecules* 30:4945
- [21] Walter H, Muller-Buschbaum P, Gutmann JS, Lorenz-Haas C, Harrats C, Jérôme R, Stamm M (1999) *Langmuir* 15:6984
- [22] Diehl A, Barbosa MC, Levin Y (1996) *Phys Rev E* 54:6516
- [23] Dobrynin AV, Rubinstein M, Joanny J-F (1998) *J Chem Phys* 109:9172
- [24] Harrison IM, Candau F, Zana R (1999) *Colloid Polym Sci* 277:48
- [25] Kamiyama Y, Israelachvili J (1992) *Macromolecules* 25:5081
- [26] Joanny J-F (1994) *J Phys II* 4:1281
- [27] Netz RR, Joanny J-F (1998) *Macromolecules* 31:5123
- [28] Blaakmeer J, Cohen-Stuart MA, Fleer GJ (1990) *J Colloid Interface Sci* 140:314
- [29] Neyret S, Ouali L, Candau F, Pefferkorn E (1995) *J Colloid Interface Sci* 176:86
- [30] Walter H, Harrats C, Muller-Buschbaum P, Jérôme R, Stamm M (1999) *Langmuir* 15:1260
- [31] Mahltig B, Walter H, Harrats C, Muller-Buschbaum P, Jérôme R, Stamm M (1999) *Phys Chem Chem Phys* 1:3853
- [32] Creutz S, Teyssié P, Jérôme R (1997) *Macromolecules* 30:6
- [33] Antoun S, Teyssié P, Jérôme R (1997) *Macromolecules* 30:1556
- [34] Creutz SV, Stam J, Antoun S, De Schryver FC, Jérôme R (1997) *Macromolecules* 30:4078
- [35] Motschmann H, Stamm M, Toprakcioglu C (1991) *Macromolecules* 24:3681
- [36] Azzam RMA, Bashara NM (1987) *Ellipsometry and polarized light*. North Holland, Amsterdam
- [37] McCrackin FL, Passaglia E, Stromberg RR, Steinberg L (1963) *J Res Natl Bur Stand Sect A* 67:363
- [38] Siqueira DF, Breiner U, Stadler R, Stamm M (1995) *Langmuir* 11:1680
- [39] Jacobasch H-J, Simon F, Werner C, Bellmann C (1996) *Tech Messen* 63:439
- [40] Jacobasch H-J, Simon F, Werner C, Bellmann C (1996) *Tech Messen* 63:447
- [41] Pecora R, Berne BJ (1976) *Dynamic light scattering*. Wiley, New York
- [42] Förster S, Schmidt M, Antonietti M (1990) *Polymer* 31:781
- [43] Briham EO (1995) *FFT: Schnelle Fourier transformation*. Oldenbourg, Munich
- [44] Gutmann GS, Muller-Buschbaum P, Stamm M (1999) *Faraday Discuss* 112:285
- [45] van de Steeg HGM, Cohen Stuart MA, de Keizer A, Bijsterbosch BH (1992) *Langmuir* 8:2538
- [46] Atkins PW (1982) *Physical chemistry*. Oxford University Press, Oxford